Journal of the Korean Ceramic Society
Vol. 48, No. 5, pp. 379~383, 2011.

http://dx.doi.org/10.4191/kcers.2011.48.5.379

Synthesis of One-dimensional Spinel $LiMn_2O_4$ Nanostructures as a Positive Electrode in Lithium Ion Battery

Hyun-Wook Lee, P. Muralidharan, and Do Kyung Kim†

Department of Materials Science and Engineering, KAIST, Daejeon 305-701, Korea

(Received August 12, 2011; Revised August 31, 2011; Accepted September 1, 2011)

ABSTRACT

This paper presents the synthesis of one-dimensional spinel $LiMn_2O_4$ nanostructures using a facile and scalable two-step process. $LiMn_2O_4$ nanorods with average diameter of 100 nm and length of 1.5 μm have been prepared by solid-state lithiation of hydrothermally synthesized β-MnO_2 nanorods. $LiMn_2O_4$ nanowires with diameter of 10 nm and length of several micrometers have been fabricated via solid-state lithiation of β-MnO_2 nanowires. The precursors have been lithiated with LiOH and reaction temperature and pressure have been controlled. The complete structural transformation to cubic phase and the maintenance of 1-D nanostructure morphology have been evaluated by XRD, SEM, and TEM analysis. The size distribution of the spinel $LiMn_2O_4$ nanorods/wires has been similar to the MnO_2 precursors. By control of reaction pressure, cubic 1-D spinel $LiMn_2O_4$ nanostructures have been fabricated from tetragonal MnO_2 precursors even below 500ºC.

Key words : Energy storage, Lithium ion battery, Lithium manganese oxide, Nanowire, Nanorod

1. Introduction

Lithium ion batteries for advanced energy storage systems have been extensively studied due to the climate-change concerns and ever growing global energy demands.[1-3] Various strategies such as nanosized materials,[4,5] doping,[6] core-shell design,[7] polyanionic materials,[8,9] anion doping with F^- and S^{2-} on the O^{2-} sites,[10,11] other alkali cations,[12,13] and different electrolyte systems have been employed to improve the performance of Lithium ion batteries.[14-16] In our previous works,[17,18] we demonstrated that the one-dimensional (1-D) nanosized cathode materials have superior rate performance than the commercial micron-sized powder due to larger contact area with the electrolyte, shorter distance for lithium ion transport, and higher electronic pathway. In addition, 1-D nanosized structure may improve the mechanical stability of the electrode compared to zero-dimensional nanosized systems which tend to undergo decrepitation during electrochemical reactions.[4]

In $LiMn_2O_4$ nanosized systems, synthetic procedures are generally complex, cost affected, and difficult to scale up. A number of soft chemistry techniques such as sol-gel,[19] solution-phase,[20] combustion,[21] and templating methods[22] have been explored to prepare $LiMn_2O_4$. Moreover, electrochemical performances of the electrode materials are closely associated with the preparation methods.[2] $LiMn_2O_4$ prepared by the traditional solid-state reaction method exhibits good performance but it requires prolonged high temperature calcination of 800ºC, which causes coarsening of the powders.[23-25] Thus, a simple and convenient route to synthesize $LiMn_2O_4$ nanostructures without loss of electrochemical properties is highly desired.

Alpha manganese oxide (α-MnO_2) and beta manganese oxide (β-MnO_2) were reported to have a particular anisotropic morphology, which can be synthesized as nanowires and nanorods of 5-10 nm and 50-100 nm diameters respectively.[26] Hence, they have been considered as possible precursors for $LiMn_2O_4$ nanosized materials,[27] but often the low crystallinity of α-MnO_2 affects the grain size distribution of the lithiated phase and the maintaining of α-MnO_2 precursor nanowire morphology during phase transformation is a formidable challenge. In this paper, we report on the synthesis of 1-D spinel $LiMn_2O_4$ nanostructures using α-MnO_2 nanowires and β-MnO_2 nanorods as precursors. The two-step synthetic process is facile and easy to scale up. It involves hydrothermal reaction to prepare β-MnO_2 nanorods and solvothermal reaction to prepare α-MnO_2 nanowires, followed by solid-state reaction with LiOH. Reaction temperature and pressure have been controlled for the successful fabrication of 1-D $LiMn_2O_4$ nanostructures maintaining precursor morphologies.

2. Experimental Procedure

Manganese oxide (MnO_2) nanostructures were synthesized by either hydrothermal or solvothermal reaction by use of deionized water (DI-water) and 1-octanol. For the synthesis of β-MnO_2 nanorods, analytical grade hydrate manganese acetate ($Mn(CH_3COO)_2 \cdot 4H_2O$, 98% Aldrich) and an equal amount of sodium persulfate ($Na_2S_2O_8$, 99.99% Aldrich) were added to DI-water and stirred to form a homogeneous clear solution. The solution mixture was then transferred

†Corresponding author : Do Kyung Kim
E-mail : dkkim@kaist.ac.kr
Tel : +82-42-350-4118 Fax : +82-42-350-3310

into a 100 mL Teflon-lined stainless steel autoclave for hydrothermal reaction to proceed at 120ºC for 12 h. After this step, the final precipitated product was washed sequentially with DI-water and ethanol to remove unreacted ions. The obtained powder was subsequently dried at 100ºC for 12 h in air. Similar process was followed to prepare α-MnO_2 nanowires. A mixture of $Mn(CH_3COO)_2{\cdot}4H_2O$ and ammonium persulfate ($(NH_4)_2S_2O_8$) with molar ratio of 1 : 1 were dissolved in DI-water. Then, ammonium sulfate ($(NH_4)_2SO_4$) was added to the mixture followed by the addition of 1-octanol. The dissolved solution was then heat treated at 140ºC for 12 h.

The synthesis of $LiMn_2O_4$ nanorods was as follows: as-synthesized β-MnO_2 nanorods and lithium hydroxide monohydrate ($LiOH{\cdot}H_2O$, 98% Junsei) were dispersed in high purity ethanol to form thick slurry, and ground to a fine mixture and dried at 60ºC. The well-mixed powder was calcined at various temperatures such as 650, 700 and 750ºC in air for 10 h. Similarly, for the synthesis of $LiMn_2O_4$ nanowires, the as-synthesized α-MnO_2 nanowires and $LiOH{\cdot}H_2O$ were mixed in high purity ethanol, and then sonicated for several hours to form a homogeneous mixture and evaporate ethanol simultaneously. Finally, the well-mixed powder was transferred into a furnace and calcined at 450ºC at low pressure in oxygen atmosphere (2 mbar). Oxygen gas was purged into the furnace to burn out the organic impurities, carbon, and nitrogen.

The synthesized nanostructures were characterized by use of an X-ray diffractometer (XRD, Rigaku, D/MAX-IIIC X-ray diffractometer, Tokyo, Japan) with Cu-Kα radiation (λ = 1.5406 Å) operating at 40 kV and 45 mA. The morphology of the nanostructures was observed by use of field emission scanning electron microscope (FE-SEM, Hitachi S-4800) and field-emission transmission electron microscope (FE-TEM, Tecnai G² F30 S-Twin). Bright field image, high-resolution TEM (HR-TEM), and diffraction factor were also used to reveal the morphology and the structure of α-MnO_2 and $LiMn_2O_4$ specimens.

3. Results and Discussion

The α and β MnO_2 nanostructures were synthesized via solvothermal and hydrothermal processes, respectively. These nanowires and nanorods are precursor materials for 1-D $LiMn_2O_4$ nanostructures. Since spinel $LiMn_2O_4$ has an isotropic cubic structure, its 1-D fabrication as nanowires and nanorods appears to be a difficult task because isotropic structure cannot grow in an anisotropic morphology using one-step reaction. For β-MnO_2 nanorods, $Na_2S_2O_8$ was used as an oxidizing reagent for $Mn(CH_3COO)_2{\cdot}4H_2O$. Similarly, α-$MnO_2$ nanowires were fabricated by use of $(NH_4)_2S_2O_8$ as an oxidizing reagent. According to the cation size of oxidizing reagent, MnO_6 tetrahedron forms (1 × 1) or (2 × 2) channel structure.[26] To fabricate thinner wire and achieve higher crystallinity, 1-octanol was added as a surfactant that prevents particle agglomeration.

Powder X-ray diffraction patterns of the prepared β and α-MnO_2 are shown in Fig. 1(a) and (b), respectively. Synthesized β-MnO_2 corresponding to JCPDS data No. 24-0735 has tetragonal phase ($P4_2/mnm$, space group 136). α-MnO_2 is indexed to a

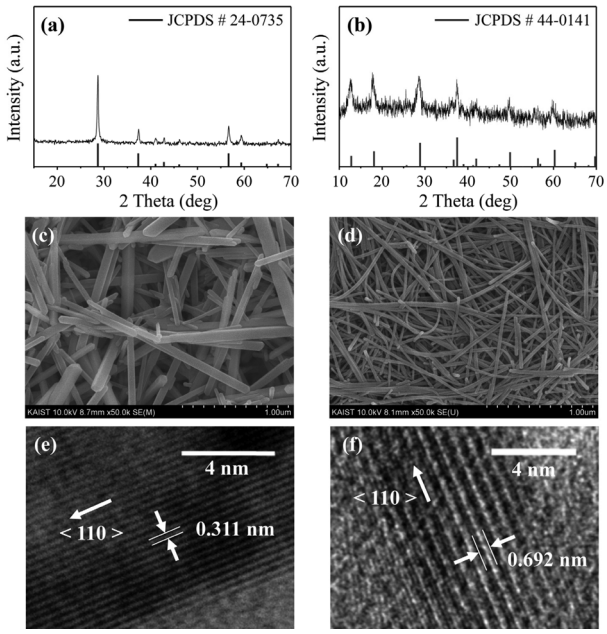

Fig. 1. Powder X-ray diffraction patterns, SEM, and HR-TEM images of as-synthesized β-MnO_2 nanorods (a, c, and e) and α-MnO_2 nanowires (b, d, and f).

pure tetragonal phase (I4/m, space group 87), which corresponds to JCPDS data No. 44-0141. The morphologies of the two nanostructures are evaluated by the FE-SEM images (Fig. 1(c) and (d)). In Fig. 1(c), the morphology of β-MnO_2 nanorods is cuboid with a diameter of 80 nm and a length of 1.5 μm, while well-dispersed α-MnO_2 nanowires have homogeneous diameter of 8 or 9 nm and lengths of several micrometers. In order to demonstrate different lattice fringes of d-spacing, HR-TEM was performed on the two specimens. The d-spacing of β-MnO_2 nanorods in Fig. 1(e) is calculated as 0.311 nm, and the lattice spacing of 0.692 nm in Fig. 1(f) is consistent with that of the α-MnO_2 (110) plane.

The $LiMn_2O_4$ nanorods were obtained by solid state reaction via as-synthesized β-MnO_2 nanorod precursor. To acquire effective reaction temperature on the reaction process, the nanorods homogeneously mixed with LiOH calcined at 400, 500, 600, 700, and 800ºC, respectively. The powder X-ray diffraction pattern of each process is demonstrated in Fig. 2(a) to (e). At lower reaction temperature, such as 400 and 500ºC, the main peak of (110) plane on β-MnO_2 phase were observed at 28 of 2 Theta value. The inter-atomic spacing (D value) of 18.6 of 2 theta was plotted in Fig. 2(f). D-spacing value exhibited lower than 4.72 Å at 400ºC reaction temperature, and from 500ºC, the values approximately matched with the theoretical value of 4.7564 Å, which concurred with the result of phase formation. Consequently, successful reaction temperature for spinel $LiMn_2O_4$ nanorods should be over 600 ºC at a normal atmospheric pressure condition. Although high reaction temperature such as 800ºC, gives higher crystallinity by XRD data, the morphology of nanorods also should be considered. Fig. 3 displays SEM images of as-synthesized $LiMn_2O_4$ nan-

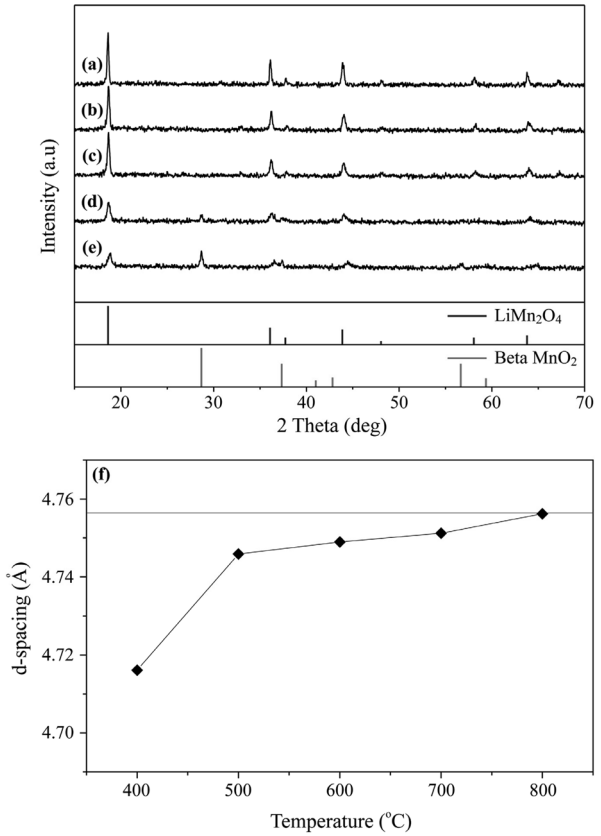

Fig. 2. XRD patterns to identify structural formation of $LiMn_2O_4$ nanorods. Solid-state reaction temperature at (a) 800, (b) 700, (c) 600, (d) 500, and (e) 400°C, respectively. (f) D-spacing plot of 18.6° on XRD data as a function of reaction temperature.

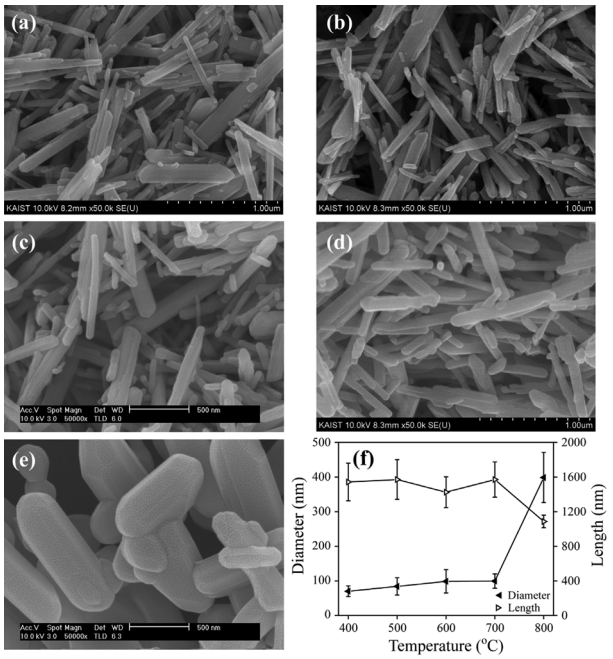

Fig. 3. SEM images of as-synthesized $LiMn_2O_4$ nanorods at (a) 400, (b) 500, (c) 600, (d) 700, and (e) 800 °C, respectively. (f) Change in average diameters and lengths of the nanorods as a function of the reaction temperature.

orods. The synthesized $LiMn_2O_4$ nanorods retained the shape of β-MnO_2 precursor under the reaction temperature of 700°C. However, at 800°C, the diameter of nanorods increased 4 times in comparison to other nanorod specimens. The changes in nanorod diameter and length after solid state reaction as a function of reaction temperature (400, 500, 600, 700, and 800°C), are shown in Fig. 3(f). According to the XRD data and SEM images, we conclude that the adequate reaction temperatures for $LiMn_2O_4$ nanorods are found to be around 600 or 700°C.

During this reaction, lithium diffuses to β-MnO_2 nanorod surface, resulting in the conversion of the structure to spinel phase $LiMn_2O_4$. It involved a major change in the oxygen arrangement from tetragonal packing to cubic close-packing.[28] To better understand the cause of this phase transformation from tetragonal to spinel cubic structure, β-MnO_2 nanorods *per se* were heat-treated at 700 °C. After heat-treatment, rutile β-MnO_2 was completely transformed to cubic spinel Mn_2O_3 while retaining its morphology (Fig. 4). As a result, β-MnO_2 nanorods undergo spontaneous phase conversion over 600°C, and simultaneously lithium ion is able to lithiate into the structure.

On the other hand, synthesis of $LiMn_2O_4$ nanowires is considerably difficult since α-MnO_2 is easily destroyed over 500°C. As mentioned above, to produce single phase $LiMn_2O_4$, solid state reaction temperature over 600°C is not acceptable. When we synthesized $LiMn_2O_4$ by use of α-MnO_2 nanowires following the same procedure of $LiMn_2O_4$ nanorods, nanowire structure did not maintain the original shape (Fig. 5). Thus, for the complete phase transformation, we modified other parameters. A stable system in thermodynamics is decided by constant temperature and pressure, and these parameters are able to modify the possible reaction value of Gibbs free energy. Thus, for the synthesis of $LiMn_2O_4$ nanowires, the reaction temperature should be under 500°C. Therefore, controlling the reaction pressure is proposed as an alternative option.

The peak intensity of XRD patterns in α-MnO_2 is relatively lower than that of $LiMn_2O_4$ or β-MnO_2. To determine whether the precursor materials exist in the final product, we examined high crystalline β-MnO_2 nanorods as a precursor material. Fig. 6 demonstrates the effect of reaction pressure at 450°C. At atmospheric pressure (760 Torr), the main peak of the precursor is present (asterisk in Fig. 6). However, when the pressure was decreased to 5, 1.5, or 0.12 Torr, the XRD patterns of the precursor material disappeared completely. Likewise, $LiMn_2O_4$ nanowires obtained via solvothermally synthesized α-MnO_2 nanowires were fabricated by controlling the pressure at 1.5 Torr and 450°C. The XRD diffracttogram of $LiMn_2O_4$ nanowires in Fig. 7(a) shows the feature of spinel structure with cubic phase (*F*d3m, space group 227, JCPDS data No. 35-0782). No peaks of the β-MnO_2 precursor phase and other impurities were detected. Fig. 7(b) and (c) show the SEM image and HR-TEM image of the nanowires. The cubic spinel $LiMn_2O_4$ nanowires were well dispersed and retained the dimensions and morphology of α-MnO_2 nanowire precursor. In Fig. 7(d), fast Fourier transforms (FFT) analysis was per-

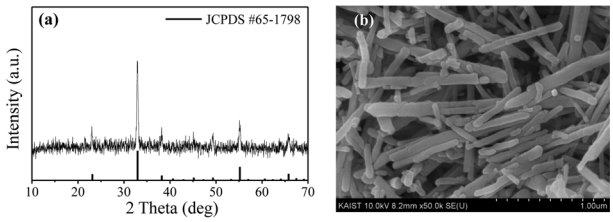

Fig. 4. (a) XRD pattern and (b) SEM images of spinel Mn_2O_3 nanorods as obtained by heat-treatment of β-MnO_2 nanorods *per se*.

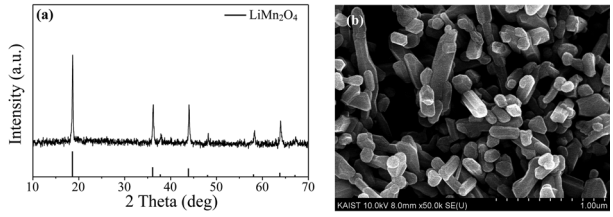

Fig. 5. (a) XRD pattern and (b) SEM images of synthesized $LiMn_2O_4$ via α-MnO_2 nanowire precursor at 700°C.

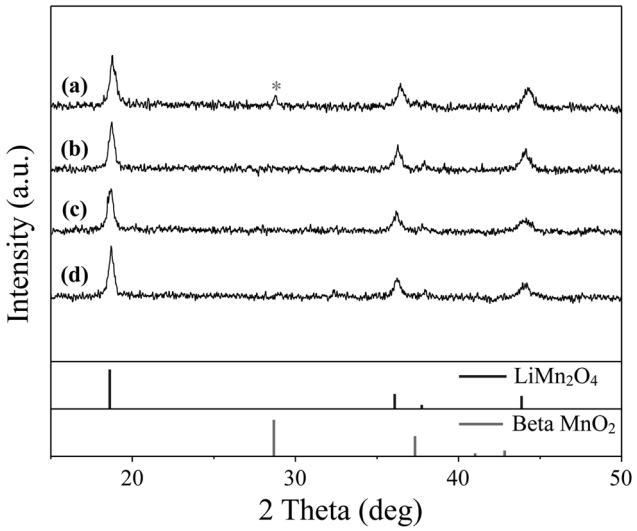

Fig. 6. XRD patterns to identify structural formation of $LiMn_2O_4$ nanorods controlled by reaction pressure. The pressure value is (a) 760, (b) 5, (c) 1.5, and (d) 0.12 Torr, respectively.

formed on the lattice fringe from the Fig. 7(c). The diffraction spots well match the [220] lattice direction of $LiMn_2O_4$ revealing single crystalline nanowires. This indicates that the solid state lithiation process in controlled temperature and prssure was able to change the phase from tetragonal structure of α-MnO_2 to cubic structure of spinel $LiMn_2O_4$ without changing the nanowire morphology and size.

4. Conclusion

$LiMn_2O_4$ nanorods and nanowires with cubic spinel structures have been fabricated from 1-D β and α-MnO_2 nanostructures, respectively. The β and α-MnO_2 nanostructures have been

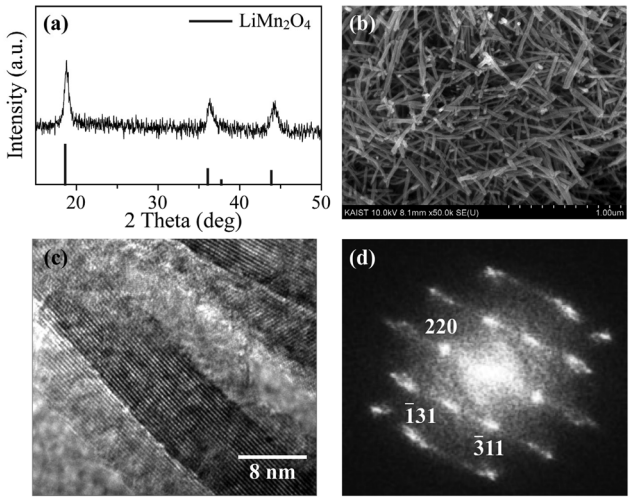

Fig. 7. (a) XRD pattern, (b) SEM, and (c) HR-TEM images of $LiMn_2O_4$ nanowires synthesized by solid state reaction between the prepared α-MnO_2 nanowires and LiOH at 1.5 Torr. (d) FFT analysis of the lattice fringes in (g).

obtained by inexpensive and scalable hydrothermal and solvothermal synthesis methods. The complete structural transformation to cubic phase and the maintenance of 1-D nanostructure morphology have both been proved by XRD data, SEM, and TEM images. We have found that the required reaction temperature for the synthesis of $LiMn_2O_4$ nanorods at normal atmospheric pressure should be more than 500°C and less than 800°C. $LiMn_2O_4$ nanowires have been fabricated at controlled pressure since the morphology of α-MnO_2 precursor will not be retained over 500°C. As produced $LiMn_2O_4$ nanorods and nanowires have been similar in size with the precursors. By controlling the pressure, cubic 1-D spinel $LiMn_2O_4$ nanostructures have been well fabricated from tetragonal MnO_2 precursors even under 500 °C reaction temperature.

Acknowledgments

The work was supported by the Green Science Project of the Research Institute of Industrial Science & Technology, the Center for Inorganic Photovoltaic Materials (No. 2011-0001001), and the National Research Foundation of Korea (NRF) funded by the Ministry of Education, Science and Technology (MEST) (NRF-2010-C1AAA001-2010-0029031). Mr. Lee was financially supported by the Priority Research Centers Program through the NRF funded by MEST (2009-0094041).

REFERENCES

1. J. M. Tarascon and M. Armand, "Issues and Challenges Facing Rechargeable Lithium Batteries," *Nature*, **414** [6861] 359-67 (2001).
2. M. S. Whittingham, "Lithium Batteries and Cathode Materials," *Chem. Rev.*, **104** [10] 4271-301 (2004).
3. B. L. Ellis, K. T. Lee, and L. F. Nazar, "Positive Electrode Materials for Li-Ion and Li-Batteries," *Chem. Mater.*, **22** [3]

691-714 (2010).
4. C. K. Chan, H. Peng, G. Liu, K. Mcilwrath, X. F. Zhang, R. A. Huggins, and Y. Cui, "High Performance Lithium Battery Anodes Using Silicon Nanowires," *Nature Nanotech.*, **3** [1] 31-5 (2008).
5. S.-W. Kim, H.-W. Lee, P. Muralidharan, D.-H. Seo, W.-S. Yoon, D. K. Kim, and K. Kang, "Electrochemical Performance and *ex situ* Analysis of $ZnMn_2O_4$ Nanowires as Anode Materials for Lithium Rechargeable Batteries," *Nano Res.*, **4** [5] 505-10 (2011).
6. B.-H. Choi, D.-J. Lee, M.-J. Ji, Y.-J. Kwon, and S.-T. Park, "Study of the Electrochemical Properties of $Li_4Ti_5O_{12}$ Doped with Ba and Sr Anodes for Lithium-Ion Secondary Batteries," *J. Kor. Ceram. Soc.*, **47** [6] 638-42 (2010).
7. Y.-K. Sun, S.-T. Myung, B.-C. Park, J. Prakash, I. Belharouak, and K. Amine, "High-energy Cathode Material for Long-life and Safe Lithium Batteries," *Nat. Mater.*, **8** [4] 320-24 (2009).
8. S.-Y. Chung, J. T. Bloking, and Y.-M. Chiang, "Electronically Conductive Phospho-olivines as Lithium Storage Electrodes," *Nat. Mater.*, **1** [2] 123-28 (2002).
9. V. Legagneur, Y. An, A. Mosbah, R. Portal, A. Le Gal La Salle, A. Verbaere, D. Guyomard, and Y. Piffard, "$LiMBO_3$ (M = Mn, Fe, Co): Synthesis, Crystal Structure and Lithium Deinsertion/insertion Properties," *Solid State Ionics*, **139** [1-2] 37-46 (2001).
10. A. R. Naghash and J. Y. Lee, "Lithium Nickel Oxyfluoride ($Li_{1-z}Ni_{1+z}F_yO_{2-y}$) and Lithium Magnesium Nickel Oxide ($Li_{1-z}(Mg_xNi_{1-x})_{(1+z)}O_2$) Cathodes for Lithium Rechargeable Batteries II. Electrochemical Investigations," *Electrochim. Acta*, **46** [15] 2293-304 (2001).
11. S. H. Park, Y. K. Sun, K. S. Park, K. S. Nahm, Y. S. Lee, and M. Yoshio, "Synthesis and Electrochemical Properties of Lithium Nickel Oxysulfide ($LiNiS_yO_{2-y}$) Material for Lithium Secondary Batteries," *Electrochim. Acta*, **47** [11] 1721-26 (2002).
12. A. D. Tevar and J. F. Whitacre, "Relating Synthesis Conditions and Electrochemical Performance for the Sodium Intercalation Compound $Na_4Mn_9O_{18}$ in Aqueous Electrolyte," *J. Electrochem. Soc.*, **157** [7] A870-75 (2010).
13. S. Komaba, C. Takei, T. Nakayama, A. Ogata, and N. Yabuuchi. "Electrochemical Intercalation Activity of Layered $NaCrO_2$ vs. $LiCrO_2$," *Electrochem. Commun.*, **12** [3] 355-58 (2010).
14. R. Ruffo, C. Wessells, R. A. Huggins, and Y. Cui, "Electrochemical Behavior of $LiCoO_2$ as Aqueous Lithium-ion Battery Electrodes," *Electrochem. Commun.*, **11** [2] 247-49 (2009).
15. M. Galiński, A. Lewandowski, and I. Stępniak, "Ionic Liquids as Electrolytes," *Electrochim. Acta*, **51** [26] 5567-80 (2006).
16. J. Y. Song, Y. Y. Wang, and C. C. Wan, "Review of Gel-type Polymer Electrolytes for Lithium-ion Batteries," *J. Power Sources*, **77** [2] 183-97 (1999).
17. D. K. Kim, P. Muralidharan, H.-W. Lee, R. Ruffo, Y. Yang, C. K. Chan, H. Peng, R. A. Huggins, and Y. Cui, "Spinel $LiMn_2O_4$ Nanorods as Lithium Ion Battery Cathodes," *Nano Lett.*, **8** [11] 3948-52 (2008).
18. H.-W. Lee, P. Muralidharan, R. Ruffo, C. M. Mari, Y. Cui, and D. K. Kim, "Ultrathin Spinel $LiMn_2O_4$ Nanowires as High Power Cathode Materials for Li-Ion Batteries," *Nano Lett.*, **10** [10] 3852-56 (2010).
19. C. J. Curtis, J. Wang, and D. L. Schulz, "Preparation and Characterization of $LiMn_2O_4$ Spinel Nanoparticles as Cathode Materials in Secondary Li Batteries," *J. Electrochem. Soc.*, **151** [4] A590-98 (2004).
20. S. Nieto, S. B. Majumder, and R. S. Katiyar, "Improvement of the Cycleability of Nano-crystalline Lithium Manganate Cathodes by Cation Co-doping," *J. Power Sources*, **136** [1] 88-98 (2004).
21. Y.-S. Han, J.-T. Son, H.-G. Kim, and H.-T. Jung, "Combustion Synthesis of $LiMn_2O_4$ with Citric Acid and the Effect of Post-heat Treatment," *J. Kor. Ceram. Soc.*, **38** [4] 301-7 (2001).
22. N. Li, C. J. Patrissi, G. Che, and C. R. Martin, "Rate Capabilities of Nanostructured $LiMn_2O_4$ Electrodes in Aqueous Electrolyte," *J. Electrochem. Soc.*, **147** [6] 2044-49 (2000).
23. J. Cabana, T. Valdés-Solís, M. R. Palacín, J. Oró-Solé, A. Fuertes, G. Marbán, and A. B. Fuertes, "Enhanced High Rate Performance of $LiMn_2O_4$ Spinel Nanoparticles Synthesized by a Hard-template Route," *J. Power Sources*, **166** [2] 492-98 (2007).
24. M. Y. Song and M. Shon, "Variations of the Electrochemical Properties of $LiMn_2O_4$ with the Calcining Temperature," *J. Kor. Ceram. Soc.*, **39** [6] 523-27 (2002).
25. M. J. Ji, E. K. Kim, Y. T. Ahn, and B. H. Choi, "Crystallinity and Battery Properties of Lithium Manganese Oxide Spinel with Lithium Titanium Oxide Spinel Coating Layer on Its Surface," *J. Kor. Ceram. Soc.*, **47** [6] 633-37 (2010).
26. X. Wang and Y. Li, "Selected-Control Hydrothermal Synthesis of α- and β-MnO_2 Single Crystal Nanowires" *J. Am. Chem. Soc.*, **124** [12] 2880-81 (2002).
27. H. Fang, L. Li, Y. Yang, G. Yan, and G. Li, "Low-temperature Synthesis of Highly Crystallized $LiMn_2O_4$ from Alpha Manganese Dioxide Nanorods," *J. Power Sources*, **184** [2] 494-97 (2008).
28. W. I. F. David, M. M. Thackeray, P. G. Bruce, and J. B. Goodenough, "Lithium Insertion into β-MnO_2 and the Rutile-spinel Transformation," *Mater. Res. Bull.*, **19** [1] 99-106 (1984).